Autoxidized citronellol: free radicals as potential sparkles to ignite the fragrance induced skin sensitizing pathway

Fatma Sahli, Bertrand Vileno, Christophe Gourlaouen, Elena Giménez-Arnau

Autoxidized citronellol: free radicals as potential sparkles to ignite the fragrance induced skin sensitizing pathway.

Fatma Sahli[a], Bertrand Vileno[a], Christophe Gourlaouen[a], Elena Giménez-Arnau[a,*]

[a] Institut de Chimie, UMR 7177, CNRS, Université de Strasbourg, 4 Rue Blaise Pascal, 67000 Strasbourg, France

Corresponding author:

Elena Giménez-Arnau

E-mail address: egimenez@unistra.fr

Abstract

Citronellol, one of the most used fragrance compounds worldwide, is one ingredient of Fragrance Mix II used to assess skin allergy to fragrances in dermatitis patients. Pure citronellol is non-allergenic. Main issue is it autoxidizes when exposed to air becoming then allergenic. The increased skin sensitizing potency of air-exposed citronellol has been attributed to the hydroperoxides detected at high concentrations in the oxidation mixtures. It has been postulated that such hydroperoxides can give rise to specific antigens, although chemical mechanisms involved and the pathogenesis are far from being unraveled. Hydroperoxides are believed to react with skin proteins through mechanisms involving radical intermediates. Here, insights on the potential radicals involved in skin sensitization to citronellol hydroperoxides are given. The employed tool is a multispectroscopic approach based on (i) electron paramagnetic resonance and spin trapping, that confirmed the formation of oxygen- and carbon-radicals when exposing reconstructed human epidermis to concentrations of hydroperoxides close to those used for patch testing patients with air-oxidized citronellol; (ii) liquid chromatography-mass spectrometry, that proved the reaction with amino acids such as cysteine and histidine, known to be involved in radical processes and (iii) density functional theory calculations, that gave an overview on the preferential paths for radical degradation.

1. Introduction

Citronellol is a monoterpene alcohol found in oils of geraniums and roses with numerous attributed pharmacological activities (Santos et al., 2019). Because of its sweet roselike odor, it is also one of the most used fragrance compounds in commercial products worldwide, from perfumes and cosmetics to household detergents (Panico et al., 2019; Rastogi et al., 2001; Soo Lim et al., 2018; Wieck et al., 2018). Though, citronellol is included in the EU list of 26 compounds qualified as skin sensitizers mandatory to label in the packaging of cosmetic products and detergents when the concentration exceeds 100 ppm in rinse-off and 10 ppm in leave-on products (EU Cosmetic Regulation EC No 1223/2009, 2009). It is also one of the six ingredients of Fragrance Mix II (FMII) used to assess allergic contact dermatitis (ACD) to fragrances in dermatitis patients (Frosch et al., 2005a, 2005b). Pure citronellol is non-sensitizing (Basketter et al., 2014 Rudbäck et al., 2014). Main issue is that, as for other well-known terpene-based fragrances such as linalool and limonene, citronellol autoxidizes when exposed to air becoming then allergenic. Main contributors to the increased skin sensitizing potency of air-exposed citronellol are thought to be hydroperoxides Citr-7-OOH and Citr-6-OOH (herein referred as Citr-OOHs, Fig. 1) detected in high concentrations in the autoxidation mixtures. Rudbäck et al reported that 10 weeks autoxidation of citronellol results in a mixture containing 84% (w/w) starting material and 11.5% (w/w) Citr-OOHs (Rudbäck et al., 2014). A recent patch test study in Sweden with a total of 658 consecutive patients with suspected ACD detected positive reactions to this oxidation mixture in 0.61%-4.5% of the patients tested at 1%, 2%, 4% or 6% in petrolatum, while pure citronellol detected positive reactions in only 0.15%-0.31% of the patients when tested at 2%, 4% or 6% in petrolatum (Hagvall et al., 2020).
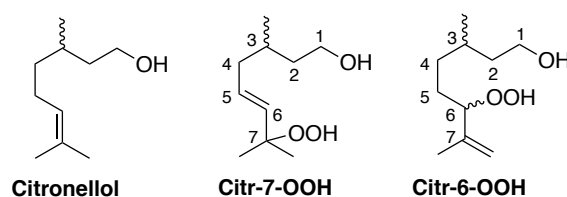

Fig. 1. Chemical structures of citronellol, Citr-7-OOH and Citr-6-OOH

ACD is a T-cell mediated delayed hypersensitivity reaction and the clinical consequence of skin sensitization, one of the most important work-related and environmental health issues associated with low molecular weight chemicals (Martin, 2015). Skin sensitization occurs through a complex multifactorial series of events. The Adverse Outcome Pathway defined by the Organization for Economic Co-operation and Development includes four key events: (KE1) binding of chemicals to proteins in the skin, (KE2) keratinocytes activation, (KE3) dendritic cells activation, and (KE4) proliferation of antigen-specific T-cells (OECD, 2014). Focusing on KE1, skin sensitizers are unable "per se" to stimulate an immune response. Immunogenicity is reached by chemical reaction with skin proteins, forming antigenic conjugates further recognized and processed for presentation to the immune system. Many chemical sensitizers are suspected to react with epidermal proteins through mechanisms involving radical intermediates, instead of the most common two electrons nucleophile-electrophile mechanism (Lepoittevin and Lafforgue, 2021). This is particularly the case of sensitizing hydroperoxides derived from autoxidation of fragrance terpenes such as limonene, linalool and citronellol. It has been postulated they can give rise to specific antigens although the pathogenesis is far from being unraveled (Karlberg et al., 2013). The parent terpenes are thus pre-haptens, as they need to be oxidized in order to become reactive and sensitizing. Current methods to assess the skin sensitizing potential of chemicals before use in consumer products (an EU mandatory issue in industry) still have gaps and lack information to forecast pre-haptens sensitization potential. Understanding the chemical mode of action is thus necessary to improve risk assessment procedures and thus help to protect both producers and consumers.

Within this context, over the last few years we have essentially based our studies on limonene and linalool hydroperoxides. We have demonstrated by electron paramagnetic resonance (EPR) combined to the spin trapping technique (ST) that easy cleavage of the O-O bond (dissociation energy *ca.* 175 kJ.mol^{-1}) of the hydroperoxides topically applied to a 3D model of reconstructed human epidermis (RHE) affords oxygen (O)-centered radicals (*i.e.*, alkoxyl, peroxyl), further undergoing radical rearrangements to form more stable carbon (C)-centered radicals in the epidermis (Kuresepi et al.,

2020; Lichter et al., 2021; For a review see Vileno et al., 2022). Evaluation of the reactivity in solution of these radicals toward amino acids prone to radical reactions showed that this intrinsic chemical reactivity could be potentially the needed trigger for the formation of the immunogenic antigen through covalent linking involving radical intermediates. We initially investigated by liquid chromatography-mass spectrometry the chemical behavior of the main allylic hydroperoxides responsible for the allergenicity of autoxidized limonene and linalool in Fe(II)/Fe(III) systems, able to degrade peroxides in vivo. We validated that C-radicals issued from these compounds alter directly the lateral chain of some of the amino acids tested (cysteine, histidine, tryptophan, lysine) and also glutathione, forming adducts via different radical processes. In parallel, due to the high oxidative strength of the media, we showed that redox processes could also be induced and generate chemical modifications on the amino acids themselves (tryptophan, tyrosine) (Kao et al., 2014, 2011). To further investigate these results, we synthesized linalool hydroperoxides containing a ^{13}C-substitution at positions precursor of C-radicals to elucidate if one of these positions could react with cysteine, its thiol chemical function being one of the most labile groups prone to react through radical mechanisms. Reactions were followed by mono- and bidimensional ^{13}C NMR. We validated that C-radicals derived from allylic hydrogen abstraction by the initially formed alkoxyl radical and/or from its β-scission can alter directly the lateral chain of cysteine forming adducts via radical processes (Kuresepi et al., 2020). Such results provided an original vision on the mechanisms likely involved in the reaction with amino acids present in the skin environment. All these findings were a step ahead toward the understanding of protein binding processes to allergenic hydroperoxides through the involvement of free radical species and thus of their sensitizing potential.

In here we have extended our investigations to the case of citronellol. We report in this manuscript evidence and mechanistic insights on derived skin sensitizing Citr-OOHs. Using a multispectroscopic approach, we evidenced (i) by EPR-ST, the formation of O- and C-radicals in RHE when exposed to concentrations of Citr-OOHs close to those used for patch testing patients with air-oxidized citronellol, (ii) by liquid chromatography combined to mass spectrometry (LC-MS), the formation of

adducts after reactivity with cysteine and histidine and (iii) by density functional theory (DFT) calculations, the potential preferential paths of radical degradation.

2. **Materials and methods**

2.1. Synthesis of compounds

2.1.1. Chemicals and materials

(±)-β-Citronellol and all other commercially available reagents were purchased from Sigma at highest available purity and used without further purification. Air and/or moisture sensitive reactions were carried out on flame dried glassware under an argon atmosphere. Dichloromethane and diethyl ether were dried on activated alumina columns under argon pressure using a dry solvent station (Glass Technology GT S100 devices). Anhydrous acetonitrile was obtained by distillation under an inert atmosphere of argon and kept on molecular sieves (4 Å). Reactions were followed by thin layer chromatography (TLC) performed on glass-backed precoated silica gel plates (Merck 60 F254). After elution, the plates were visualized under ultraviolet light (254 nm). When necessary, they were immersed in a cerium phosphomolybdic acid solution (PMA/Ce) followed by heating. PMA/Ce solution was prepared by mixing phosphomolybdic acid (2 g), cerium (IV) sulfate (0.8 g), sulfuric acid (4.8 mL) and distilled water (72.5 mL). Column chromatography purifications were carried out using silica gel 60 (Merck, Geduran, 40-63 μm) or previously neutralized silica gel. Neutralized silica was prepared by adding to a homogenous distilled water solution of silica 60 a saturated solution of sodium hydrogen carbonate up to a pH of *ca.* 8. After decantation, the silica precipitate was washed several times with water to reach a pH of *ca.* 7, filtered and dried in an oven at least for 24 h. Proton (^{1}H NMR) and carbon (^{13}C NMR) nuclear magnetic resonance spectra were recorded on Bruker Avance spectrometers at 300 MHz for ^{1}H and 75 MHz for ^{13}C or at 500 MHz for ^{1}H and 125 MHz for ^{13}C. Chemical shifts (δ) are reported in parts per million (ppm). The residual solvent peak was used as reference value. For ^{1}H NMR: CDCl$_3$ = 7.26 ppm. For ^{13}C NMR: CDCl$_3$ = 77.16 ppm. Multiplicities are indicated as s (singlet), br s (broad singlet), d (doublet), t (triplet), td (triplet of doublets) and m (multiplet). Constant couplings (J) are given in Hertz (Hz). Signal attributions were

determined either on the basis of unambiguous chemical shifts or coupling patterns. High resolution mass spectrometry (HRMS) analyses were performed on a Bruker Daltonics microTOF spectrometer (Bruker Daltonik GmgH, Bremen, Germany) equipped with an orthogonal electrospray (ESI) interface. Calibration was performed using a solution of 10 mM sodium formiate. Sample's solutions were introduced into the spectrometer source with a syringe pump (Harvard type 55 1111: Harvard Apparatus Inc., South Natick, MA, USA) with a flow rate of 4 μL.min^{-1}.

2.1.2. Synthesis of mixture 6-hydroperoxy-3,7-dimethyloct-7-en-1-ol ((±)-Citr-6-OOH) and (E)-7-hydroperoxy-3,7-dimethyloct-5-en-1-ol ((±)-Citr-7-OOH) (Sch. 1)

A microemulsion was prepared by adding sodium molybdate (2.3 g in 12 mL of distilled water) dropwise into a suspension of sodium dodecyl sulfate (19 g) in butanol (23 mL) and dichloromethane (133 mL). The microemulsion became clear after 25 min stirring. A solution of β-(±)-citronellol (3.42 g, 21.9 mmol, 1.0 eq) in the microemulsion (50 mL) was treated at room temperature with a first portion of hydrogen peroxide (30 % w/w in water, 1 mL). The brick red mixture was stirred for about 20 min until it became light yellow. Other thirteen portions of hydrogen peroxide (30 % w/w in water, 1 mL each) were successively added every 20 min. A total of 14 mL of aqueous hydrogen peroxide were used (137.1 mmol, 6.3 eq). The light-yellow mixture was stirred overnight at room temperature becoming completely clear. After this time, the solvent was removed under reduced pressure and the crude product obtained dissolved in dichloromethane (100 mL). The suspension was stirred vigorously for about 45 min and filtered. The filtrate was evaporated under reduced pressure and the recovered oil was diluted in ethyl acetate (20 mL) and washed with water (3×100 mL). The aqueous layers were extracted with ethyl acetate (3×30 mL). The organic layers were dried over magnesium sulfate, filtered and evaporated under reduced pressure. Purification by column chromatography on silica gel (petroleum ether/ethyl acetate 9:1) furnished the mixture (±)-Citr-6-OOH/(±)-Citr-7-OOH (ratio 6/4) as a yellow oil (3.4 g, 18.1 mmol, 73 % yield). Rf=0.35 (petroleum ether /ethyl acetate 6:4). CAS number: (±)-Citr-7-OOH: 81113-73-7; (±)-Citr-6-OOH: 81113-74-8. ^{1}H NMR (500 MHz, CDCl$_3$): (±)-Citr-6-OOH (mixture of two diastereoisomers): δ 0.90 (d, 6 H, *J*=6.8 Hz, 2 × CH-C*H*$_3$),

1.07-1.26 (m, 4 H, 2 × CH_2), 1.35-1.43 (m, 4 H, 2 × CH_2), 1.49-1.64 (m, 6 H, 2 × CH_2 and 2 × CH-

CH_3), 1.72 (s, 6 H, 2 × C-CH_3), 3.62-3.72 (m, 4 H, 2 × CH_2-OH), 4. 28 (td, 2 H, J=6.95 Hz, J=3.1

Hz, 2 × CH-OOH), 4.99-5.01 (m, 4 H, 2 × C-CH_2), 8.34 (br s, 1 H, -OOH), 8.40 (br s, 1 H, -OOH);

(±)-Citr-7-OOH: δ 0.89 (d, 3 H, J=6.75 Hz, CH-CH_3), 1.32 (s, 6 H, 2 × C-CH_3), 1.07-1.64 (m, 3 H,

CH-CH$_3$ and CH-CH_2), 1.93-2.09 (m, 2 H, CH_2), 3.62-3.72 (m, 2 H, CH_2-OH), 5.52- 5.56 (d, 1 H,

J=15.75 Hz, CH-C-OOH), 5.64 -5.70 (m, 1 H, CH-CH-C), 7.96 (br s, 1 H, -OOH). ^{13}C NMR (125

MHz, CDCl$_3$): (±)-Citr-6-OOH (mixture of two diastereoisomers): δ 17.2, 17.3, 19.6, 19.7, 28.1, 28.2,

29.2, 29.4, 32.8, 32.90, 39.6, 39.7, 61.12, 61.14, 89.8, 90.0, 114.3, 114.5, 143.8, 144.0; (±)-Citr-7-

OOH: δ 19.9, 24.5 (2C), 29.7, 39.2, 39.9, 61.1, 82.2, 130.2, 135.1.

2.1.3   Synthesis of (E)-7-hydroperoxy-3,7-dimethyloct-5-en-1-ol ((±)-Citr-7-OOH) (Sch. 2)

3,7-Dimethyloct-6-en-1-yl acetate (1): A solution of (±)-β-citronellol (5.0 g, 32.0 mmol, 1.0 eq)

in dichloromethane (150 mL) was cooled to 0 °C and successively treated with pyridine previously

distilled (10.3 mL, 127.8 mmol, 4.0 eq), 4-(dimethylamino) pyridine (390 mg, 3.2 mmol, 0.1 eq) and

acetic anhydride (9 mL, 96.1 mmol, 3.0 eq). After stirring 45 min at this temperature, the reaction

mixture was diluted with dichloromethane (50 mL) and washed with hydrochloric acid (1M, 150

mL), distilled water (150 mL), a saturated sodium bicarbonate solution (150 mL) and brine (150 mL).

Combined organic layers were dried over magnesium sulfate and the solvent was evaporated under

reduced pressure. Purification by column chromatography on silica gel (pentane/diethyl ether 8:2)

furnished 3,7-dimethyloct-6-en-1-yl acetate as a colorless oil (5.30 g, 26.73 mmol, 84 % yield). CAS

number: 150-84-5. Rf = 0.81 (pentane/diethyl ether 8:2). ^{1}H NMR (500 MHz, CDCl$_3$): δ 0.89 (d, 3

H, J=6.7 Hz, CH-CH_3), 1.12-1.56 (m, 5 H, CH_2-CH-CH$_3$, CH-CH$_3$ and CH_2-CH$_2$), 1.58 (s, 3 H, C-

CH_3CH$_3$), 1.66 (s, 3 H, C-CH$_3$CH_3), 1.89-2.00 (m, 2 H, CH$_2$-CH_2), 2.02 (s, 3 H, COCH_3), 4.03-4.12

(m, 2 H, CH_2-O), 5.07 (t, J=7.1 Hz, 1 H, CH-C). ^{13}C NMR (125 MHz, CDCl$_3$): δ 17.2, 19.5, 21.2,

27.47, 25.8, 29.5, 35.5, 37.1, 63.1, 124.66, 131.44, 171.3.

(E)-7-Hydroxy-3,7-dimethyloct-5-en-1-yl acetate (2): A solution of diphenyl diselenide (11.8 g,

37.8 mmol, 1.5 eq) in anhydrous dichloromethane (100 mL) was cooled to 0 °C and treated with

hydrogen peroxide (35 % w/w in water, 4.0 mL, 42.0 mmol, 1.7 eq). After stirring vigorously at this temperature for 30 min, anhydrous magnesium sulfate (5.0 g, 41.5 mmol, 1.6 eq) was added and the reaction mixture stirred at 0 °C for 30 min. The ice bath was after this time removed, 3,7-dimethyloct-6-en-1-yl acetate (5.0 g, 25.2 mmol, 1.0 eq) was added and the mixture was stirred vigorously for 15 h at room temperature. The reaction mixture was then cooled down again to 0 °C and chilled *tert*-butyl hydroperoxide (15 mL, 149.1 mmol, 5.9 eq) was added. After removing the ice bath, the reaction mixture was stirred at room temperature for 20 h and filtered after this time. The filtrate was concentrated under reduced pressure. Then the orange residue was dissolved in diethyl ether (60 mL), washed with sodium carbonate (60 mL), distilled water (60 mL), sodium hydrogenocarbonate (60 mL) and brine (60 mL). Combined organic layers were dried with magnesium sulfate, filtered and concentrated under reduced pressure. Purification by column chromatography on silica gel (pentane/diethyl ether 8:2) furnished 7-hydroxy-3,7-dimethyloct-5-en-1-yl acetate as a yellow oil (4.3 g, 20.2 mmol, 80 % yield). CAS number: 91464-78-7. Rf=0.28 (pentane/diethyl ether 8:2). ^{1}H NMR (500 MHz, CDCl$_3$): δ 0.90 (d, 3 H, J= 6.7 Hz, CH-CH_3), 1.30 (s, 6 H, C-CH_3CH_3), 1.41-1.47 (m, 1 H, CH-CH$_3$), 1.59-1.69 (m, 2 H, CH_2-CH-CH$_3$), 1.88-2.06 (m, 5 H, CH_2-CH and -COCH_3), 4.05-4.13 (m, 2 H, CH_2-O), 5.54-5.64 (m, 2 H, CH-CH). ^{13}C NMR (125 MHz, CDCl$_3$): δ 19.5, 21.2, 30.0 (2C), 30.2, 35.1, 39.6, 63.0, 70.8, 125.1, 140.0, 171.4.

(E)-7-Hydroperoxy-3,7-dimethyloct-5-en-1-yl acetate (3): To an aqueous solution of hydrogen peroxide (50 % w/w in water, 140 mL) were added, at 0 °C, 10 drops of concentrated sulfuric acid and 7-hydroxy-3,7-dimethyloct-5-en-1-yl acetate (2.0 g, 9.33 mmol, 1.0 eq). The reaction mixture was vigorously stirred at 0 °C during 15 h. After this time, the reaction mixture was extracted with dichloromethane (3×100 mL). The organic layers were combined, dried over magnesium sulfate, filtered and evaporated under reduced pressure. The crude product was purified by column chromatography on neutralized silica gel (pentane/ethyl acetate 8:2) to obtain (*E*)-7-hydroperoxy-3,7-dimethyloct-5-en-1-yl acetate as a colorless oil (1.30 g, 5.60 mmol, 60 % yield). CAS number: 105987-64-2. Rf = 0.6 (pentane/diethyl ether 8:2). ^{1}H NMR (500 MHz, CDCl$_3$): δ 0.91 (d, 3 H, J=6.5

Hz, CH-CH_3), 1.33 (s, 6 H, C-CH_3CH_3), 1.41-1.48 (m, 1 H, CH-CH$_3$), 1.62-1.70 (m, 2 H, CH_2-CH-CH$_3$), 1.93-2.10 (m, 5 H, CH_2-CH and -COCH_3), 4.08-4.13 (m, 2 H, CH_2-O), 5.54-5.68 (m, 2 H, CH-CH), 7.64 (s, 1 H, -OOH). ^{13}C NMR (125 MHz, CDCl$_3$): δ 19.6, 21.2, 24.5 (2C), 30.0, 35.0, 39.7, 63.0, 82.2, 129.8, 135.4, 171.6.

(E)-7-hydroperoxy-3,7-dimethyloct-5-en-1-ol ((±)-Citr-7-OOH): A solution of (*E*)-7-hydroperoxy-3,7-dimethyloct-5-en-1-yl acetate (1.30 g, 5.60 mmol, 1.0 eq) in anhydrous methanol (25 mL) was treated with potassium carbonate (3.90 g, 28.2 mmol, 5.0 eq) and stirred for 2.5 h at room temperature. The reaction mixture was then diluted with distilled water and the aqueous layer extracted with ethyl acetate (3×50 mL). The organic layers were combined, dried over magnesium sulfate, filtered and evaporated under reduced pressure. The crude product was purified by column chromatography on neutralized silica gel (petroleum ether/ethyl acetate 6:4) to furnish (*E*)-7-hydroperoxy-3,7-dimethyloct-5-en-1-ol ((±)-Citr-7-OOH) as a colorless oil (932.6 mg, 4.95 mmol, 88 % yield). CAS number: 81113-73-7. Rf=0.33 (petroleum ether/ethyl acetate 6:4). HRMS (ESI): *m/z* calculated for C$_{10}$H$_{20}$O$_3$ [M + Na]$^+$: 211.12 ; found : 211.13. ^{1}H NMR (500 MHz, CDCl$_3$): δ 0.91 (d, 3 H, *J*=6.7 Hz, CH-CH_3), 1.33 (s, 6 H, C-CH_3CH_3), 1.36-1.43 (m, 1 H, CH-CH$_3$), 1.58-1.78 (m, 2 H, CH_2-CH-CH$_3$), 1.93-2.09 (m, 2 H, CH_2-CH), 3.63-3.73 (m, 2 H, CH_2-OH), 5.53-5.70 (m, 2 H, CH-CH), 7.78 (s, 1 H, -OOH). ^{13}C NMR (125 MHz, CDCl$_3$): δ 19.9, 24.5 (2C), 29.7, 39.2, 39.9, 61.1, 82.2, 129.8, 135.4.

2.2. EPR spin trapping

Most of free radicals in biological systems are not directly detectable by conventional EPR, in particular because of their extremely short lifetime (milliseconds to nanoseconds), in line with their high reactivity. To overcome this pitfall, an "indirect" detection approach a.k.a spin trapping (ST) is then employed: a diamagnetic molecule "the trap" reacts with the probed radical leading to a persistent paramagnetic spin adduct whose EPR signature is linked to the nature of the trapped species (Lauricella and Tuccio, 2020). Herein the spin trap used is 5-diethoxyphosphoryl-5-methyl-1-pyrroline N-oxide (DEPMPO) that was synthesized as reported in the literature (Barbati et al., 1997).

In this case, spin adducts are formed by addition of transient radicals to the α position of the nitronyl group of DEPMPO (Supplementary Material S.1). In the case of ACD, an EPR-ST method was established "from the molecule to the tissue" using EpiSkin™ RHE as skin model (Kuresepi et al., 2020, 2018; Lichter et al., 2021; Sahli et al., 2019a; Vileno et al., 2022). Prior to the RHE investigation, a preliminary study was carried out in solution aiming at determining the nature of the radicals formed in a minimal system when compared to the skin environment. This allows to optimize the experimental conditions (choice of the spin trap, signal-to-noise ratio (S/N) …), keeping the Citr-OOHs as low as possible such as for real life exposure scenarios. Experimental protocols for EPR-ST studies were based on previous work (Sahli et al., 2019b).

2.2.1. *Studies in solution*

Radical initiation is triggered by a Fenton-type reaction induced by Fe(II) (ferrous sulfate heptahydrate, $FeSO_4$-$7H_2O$) in catalytic quantities regarding the target molecule concentration. Reactions were performed in HEPES buffer (pH 6.8; 10 mM) prepared with 1.19 g HEPES in 400 mL of deionized water, 4 g NaCl and 0.1 g KCl. pH was finally tuned by careful addition of strong base (NaOH pellets) and acid (HCl). Deionized water was added until a final volume of 500 mL. EPR spectra were recorded on an EPR X-band spectrometer (ESP300E, Bruker Biospin GmbH, Germany) equipped with a high sensitivity resonator (4119HS-W1, Bruker Biospin GmbH, Germany). The *g* calibration was performed using Bruker standard (strong pitch) with known isotropic *g* factor of 2.0028. The principal experimental parameters values were microwave frequency of ca. 9.8 GHz, microwave power 5 mW, modulation amplitude 1 G, time constant of ca. 80 ms, conversion time of ca. 160 ms. Spectra were recorded at room temperature (295 K ±1 K). All experimental EPR spectra were analyzed by means of computer simulation using labmade scripts based on Easyspin toolbox under Matlab (Mathworks) environment (Stoll and Schweiger, 2006).

As a general procedure, stock solutions were prepared for the hydroperoxides (10 mM, HEPES/CH_3CN 9:1), DEPMPO (100 mM in HEPES) and $FeSO_4$.$7H_2O$ (10 mM in HEPES). 25 μL of DEPMPO solution were mixed with $FeSO_4$.$7H_2O$ (i.e., 0.5 μL for a final concentration in the

reaction mixture of 0.1 mM), 5 μL hydroperoxide solution added and the final volume completed to 50 μL. This way, final concentrations in the reaction mixture were 50 mM DEPMPO, 1 mM target compound and 0.1 mM Fe(II). The reaction mixture was subjected to stirring, further introduced into an EPR glass capillary (Hirschamn, 25 μL), sealed on both ends and transferred forthwith in the EPR cavity for measurement.

2.2.2. Studies in reconstructed human epidermis

EpiSkin™ (0.38 cm² small format, Lyon, France) is an *ex vivo* reconstructed human epidermis (RHE) from normal human keratinocytes cultured for 13 days on a collagen matrix at the air-liquid interface. Immediately after arrival, the RHE were removed from the agarose-nutrient solution in the shipping multiwell plate under a sterile airflow and immediately placed in a plate in which each well was previously filled with 2 mL EpiSkin™ maintenance medium at room temperature. Samples were placed in the incubator at 37 °C, 5 % CO_2 and saturated humidity at least 24 h before incubation.

As a general procedure, the RHE were first of all pre-treated with DEPMPO in dimethylsulfoxide/HEPES 1:1 (250 mM, 20 μL) and incubated during 15 min (37 °C, 5 % CO_2). After this time, pre-treated RHE were placed in an EPR tissue cell equipped with a silica window (Willmad, #ER162TC-Q) and the hydroperoxides (100 mM, 50 mM, 25 mM, 10 mM or 5 mM in acetone, 20 μL) were topically applied to the RHE taking care to ensure that the solution was only applied to it. EPR spectra were then recorded forthwith using the previously depicted equipment. In here, the principal experimental parameters values were: microwave frequency of ca. 9.8 GHz, microwave power 5 mW, modulation amplitude 1 G, time constant of ca. 160 ms, conversion time of ca. 320 ms, resulting in ca. 5 minutes acquisition for a single scan and up to 10 scans were accumulated to achieve reasonable S/N. No Fe(II) was added in RHE experiments, indicating that Citr-OOHs radical initiation has been induced by the RHE itself.

2.3. Computational DFT

Calculation studies were completed by means of Gaussian 09 package (Gaussian 2009, version D.01) at Density Functional level of Theory (DFT) with ωB97XD functional. Atoms were described

by the 6-31+G** basis set (Ditchfield et al., 1971), and water solvent modeled through a polarized continuum model (Cossi et al., 1996). Structures were optimized and the nature of the encountered stationary point categorized by a frequency calculation. The minima connected by a transition state were checked by an intrinsic reaction coordinate calculation following the imaginary frequency. Gibbs free energies were extracted from the frequency calculation done within the harmonic approximation. For each studied hydroperoxide the energy reference is the initial alkoxyl radical.

2.4. Reactivity with amino acids

N-Terminal ends of the amino acids were acetylated and carboxylic groups in an ester form to avoid any secondary reactions and to simulate their function in a peptide sequence, leaving the side chain free and thus potentially reactive. Amino acids tested were *N*-Ac-Cys-COOMe, *N*-Ac-Tyr-COOEt, *N*-Ac-Trp-COOEt and *N*-Ac-His-COOMe. They were purchased from Sigma, except for *N*-Ac-His-COOMe that we synthesized (Supplementary Material S.2).

Citr-7-OOH (100 mg, 1.0 eq) was dissolved in 15 mL deaerated H_2O/acetonitrile (1:1 (v/v)). An excess of amino acid (188 mg *N*-Ac-Cys-COOMe, 267 mg *N*-Ac-Tyr-COOEt, 291 mg for *N*-Ac-Trp-COOEt, 224 mg *N*-Ac-His-COOMe; 2.0 eq) was then added together with a catalytic amount of $FeSO_4.7H_2O$ (10 mg, 0.1 eq) for radical initiation. The reaction mixture was stirred at room temperature, hidden from light and under an argon atmosphere to minimize competing reactions with oxygen. The reaction was monitored by TLC glass-backed precoated silica gel plates (Merck 60 F254). After migration, TLC plates were inspected under UV light (254 nm) then sprayed with the earlier described phosphomolybdic acid solution, followed by heating. The reaction was stopped after seven days as it was not progressing anymore even if the hydroperoxide was still present. The mixture was filtered on Celite 545 to remove iron salts and the filtrate solvent removed under reduced pressure. The obtained crude was then analyzed by liquid chromatography electrospray ionization tandem mass spectrometry (LC/ESI-MS/MS) performed with an Agilent 1200 HPLC system connected to an ion trap mass Agilent QToF spectrometer. Samples were subjected to reverse phase chromatography on a Zorbax SB-C18 column (50 mm × 2.1 mm, 1.8 μm particle size) at a flow rate
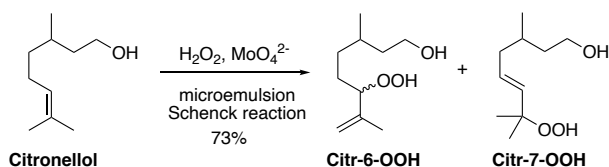
of 0.5 mL/min. They were eluted from the column using a mobile phase A (0.05% formic acid in acetonitrile) and a mobile phase B (0.05% formic acid in H_2O) with the gradient: started at 98% B and decreased to 0% B after 8 min, kept at 0% B during 12.5 min, and increased again to 98% B after 12.5 min, kept at 98% B during 13 min at the end. After passing through the diode array absorbance detector, the eluent was directed to the connected ion trap mass spectrometer with a standard electrospray source. The ionization method used was ESI in the positive ion mode (heated capillary temperature 340 °C, gas flow 8 L.min^{-1}, nebulizer gas 30 psi). Full scan mass spectra were acquired in the profile mode scanning *m/z* 50 to 1000. For ESI-MS/MS studies, the mass spectrometer was equipped with the ESI source used for ESI-MS studies described above and with the same source parameter settings. The ionization mode was ESI in the positive ion mode. The isolation width was 4 *m/z*. Data were processed using the Agilent Mass Hunter Qualitative Analysis software. Only molecular ions detected by LC-ESI-MS having an *m/z* value in accordance with potential adducts were considered. Even if unlikely, the eventuality of these ions being fragments of other molecular species cannot be excluded.

3. Results

3.1. Synthesis of compounds

The production of Citr-6-OOH and Citr-7-OOH by autoxidation of citronellol is not always reproducible, but more importantly low yields are obtained and isolation-purification from the oxidation mixtures is an arduous task. In order to carry out our studies, it was necessary to develop short and reproducible synthesis routes enabling the compounds under study to be obtained.

The mixture Citr-6-OOH/Citr-7-OOH (ratio 6/4) was obtained in one single step by subjecting (±)-β-citronellol to a Schenck reaction, in which singlet oxygen was chemically generated by disproportionation of hydrogen peroxide catalyzed by sodium molybdate in a microemulsion (Aubry et al., 2006; Aubry and Cazin, 1988; Kao et al., 2011) (Sch. 1).
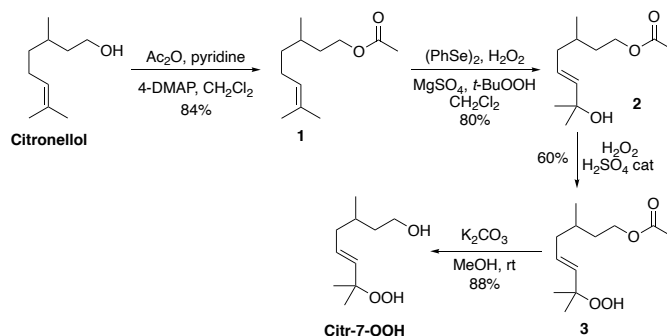
Sch. 1. Synthesis of mixture Citr-6-OOH/Citr-7-OOH (6/4)

The starting material for the synthesis being racemic (±)-β-citronellol, further derivatives were thus obtained as mixtures of isomers. However, from now on, the stereochemistry of the chiral centers present in the molecules will not be specified in the figures for simplicity reasons.

All attempts to separate both isomers were unsuccessful. Thus, we decided to synthesize each compound separately being only successful for Citr-7-OOH. As reactivity through radical intermediates was expected to be similar for both compounds (further confirmed by DFT calculations below), we kept on the studies with Citr-7-OOH comparing the results to the mixture Citr-6-OOH/Citr-7-OOH.

Citr-7-OOH was synthesized in four steps from (±)-β-citronellol as shown in Sch. 2.

Sch. 2. Synthesis of Citr-7-OOH

Citronellol alcohol function was first protected via acetylation to give **1**. Further addition of hydrogen peroxide (35% w/w aqueous solution) to diphenyl diselenide generated *in situ* phenyl selenic acid which added to the C=C bond of **1** to form a hydroxy selenide. The presence of magnesium sulfate sequestered water and allowed total Markovnikoff regioselectivity. Oxidation of the selenide by *tert*-butyl hydroperoxide gave a thermally unstable selenoxide which eliminated phenylselenic acid to give **2** (Sharpless and Lauer, 1973). Conversion of **2** into hydroperoxide **3** was

carried out by forming a stable tertiary carbocation thanks to sulfuric acid (98%) in catalytic amount and in presence of hydrogen peroxide (Lepoittevin and Karlberg, 1994). Finally, Citr-7-OOH was obtained by cleavage of the acetyl group in the presence of potassium carbonate in methanol.

3.2. EPR spin trapping

The EPR spectrum obtained with Citr-7-OOH (1 mM)/DEPMPO (50 mM)/Fe(II) (0.1 mM) is shown in Fig. 2. Simulation and deconvolution afforded spectra of spin adducts corresponding to the trapping of hydroxyl (DEPMPO-OH spin adduct), C-centered (DEPMPO-R1 and DEPMPO-R2 spin adducts) and potentially peroxyl/alkoxyl radicals (DEPMPO-OOR/OR spin adducts), with distinctive hyperfine coupling constants (*hfccs*) reported in Table 1 and in agreement with previous investigations (Dikalov et al., 2003; Frejaville et al., 1995; Karoui et al., 2011; Kuresepi et al., 2020; Vileno et al., 2022). A very similar profile to that of Citr-7-OOH was observed with the mixture Citr-6-OOH/Citr-7-OOH, yet with distinct spin adduct proportions (Supplementary Material S.3). Interestingly, peroxyl/alkoxyl radicals were not detected with the mixture.
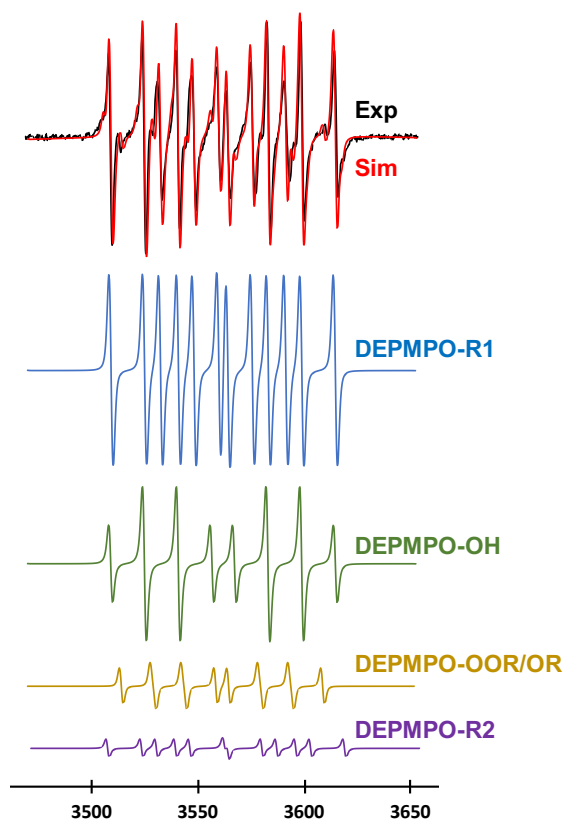
Fig. 2. EPR experimental spectrum (Exp) of Citr-7-OOH (1mM)/DEPMPO (50 mM)/Fe (II) (0.1 mM) in 10 mM HEPES solution (pH = 6.8), with overlayed computer simulation (Sim). Deconvolution afforded spectra of spin adducts DEPMPO-R1, DEPMPO-R2, DEPMPO-OH and DEPMPO-OOR/OR (*hfccs* shown in Table 1). All *g* factors were measured and found to be of *ca*. 2.0055±0.0005. Control experiments with only Citr-7-OOH or DEPMPO did not give any signal.

Experiments were then performed in RHE with topical application of the hydroperoxides to mimic real-life exposure. Treatment of RHE with the mixture Citr-6-OOH/Citr-7-OOH or with single Citr-7-OOH gave analogous conclusions. As reported for limonene and linalool hydroperoxides (Lichter et al., 2021; Kuresepi et al., 2020), concentrations of spin trap and target compounds required in RHE were much higher than those giving a decent S/N ratio signal in solution. This is probably due to RHE 3D matrices that include the *stratum corneum* influencing penetration concerns and offering various reduction pathways for both free radicals and/or spin adducts. Also, RHE content in phospholipids and ceramides may influence RHE barrier properties (Netzlaff et al., 2005). Using 250 mM DEPMPO, spin adducts started to be observed from topical application of 10 mM

hydroperoxides. Best S/N ratios were yet observed with 50 mM Citr-7-OOH and 50 mM Citr-6-OOH/Citr-7-OOH (Fig. 3).

Basically, as for the investigations in solution, fingerprints of adducts from C-centered and hydroxyl radicals trapped by DEPMPO were detected in RHE. While DEPMPO-OOR/OR testimony of peroxyl/alkoxyl radicals were observed in solution at relatively low amount, it was not the case throughout RHE studies. Yet, their presence cannot be totally excluded, as the reductive environment of the RHE decreases the lifetime of spin adducts and thus affects the corresponding S/N.
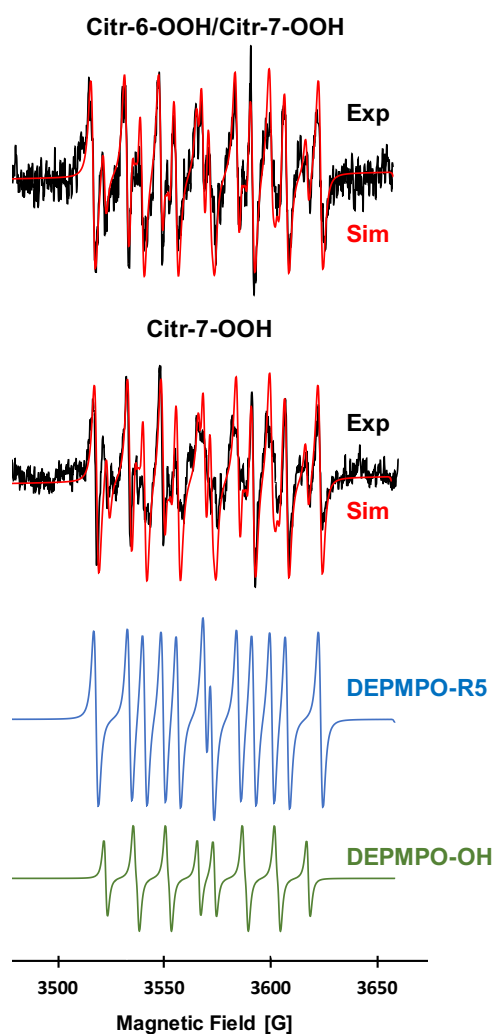

Table 1. Hyperfine coupling constants (*hfccs*) of spin adducts identified in solution and in RHE*

Spin adducts	Coupling constants**		
	a_N (G)	a_H (G)	a_P (G)
In solution			
Citr-7-OOH			
DEPMPO-OH	13.4	14.6	47.1
DEPMPO-R1	14.7	21.7	47.2
DEPMPO-R2	14.9	21.7	52.7
DEPMPO-OOR/OR	14.6	14.6	53.7
Citr-6/7-OOH***			
DEPMPO-OH	14.2	13.4	47.7
DEPMPO-R3	15.2	22.3	48.7
DEPMPO-R4	14.3	22.4	45.9
In RHE			
Citr-7-OOH			
DEPMPO-OH	14.0	12.6	46.9
DEPMPO-R5	14.5	20.8	47.7
Citr-6/7-OOH			
DEPMPO-OH	14.0	12.6	47.5
DEPMPO-R6	14.7	21.5	48.0

* *hfccs* in RHE were calculated following the best simulation attempts considering the S/N
** All *g* factors were measured and found to be of ca. 2.0055±0.0005 in solution and 2.0057±0.0005 in RHE
*** Spectra in Supplementary Material S.3

Fig. 3. EPR experimental spectra (Exp) of mixture Citr-6-OOH/Citr-7-OOH (50 mM)/DEPMPO (250 mM) and of Citr-7-OOH (50 mM)/DEPMPO (250 mM) in RHE with overlayed simulations (Sim). Very similar fingerprints were observed (Table 1). Deconvolution of the spectra afforded characteristic DEPMPO-R and DEPMPO-OH spin adducts, here shown in the case of Citr-7-OOH. All *g* factors were measured and found to be of *ca*. 2.0057±0.0005. Control experiments with only the hydroperoxides or DEPMPO did not give any signal.

3.3. Computational DFT

DFT calculations showing preferential paths for Citr-7-OOH and Citr-6-OOH radical degradation are displayed in Fig. 4 (see Supplementary Material S.4 for complete DFT results). For both compounds, the initially formed O-radical is practically in equilibrium with the epoxide species due to the small barrier between the two structures (paths A and D) and their equivalent stability. In Citr-7-OOH, two more favored paths have been identified. Path B leads to elimination of a methyl radical to form a conjugated ketone. The methyl radical can further react with the enone to form a new delocalized radical. Path C goes through a migration of H atom and this intermediate can either lead to intramolecular cyclisation (C2 and C3), or to a second rearrangement to form a conjugated radical (C1). Considering the associated barriers, paths B and C are competitive and both reactions are possible. Similarly, paths C2 and C3 are also competitive whereas the significantly higher barrier associated to C1 show that this path can be excluded. Accordingly, the evolution of the Citr-7-O˙ species leads to a mixture of cyclisation products and of conjugated enone with emission of methyl radical. No methyl radical departure is possible from Citr-6-O˙ and we have identified three competitive paths. Path E generates methacrolein by β-scission. In paths F and G, the system undergoes a migration of an H atom, followed by a second migration to give a conjugated radical (F1, F4 and G1). From F, cyclisation is also possible (F2 and F3) and is associated to a lower barrier. Again, Citr-6-O˙ radical will lead to a mixture of C-radicals located in five and six member rings as major products for kinetic considerations (lowest barriers). The conjugated radical, though being thermodynamically favored, should be a minor product, the reversibility of path F2 at room temperature being unlikely. Thus, both isomers showed a similar reactivity. We therefore assumed that they could behave similarly in the presence of amino acids in the skin.
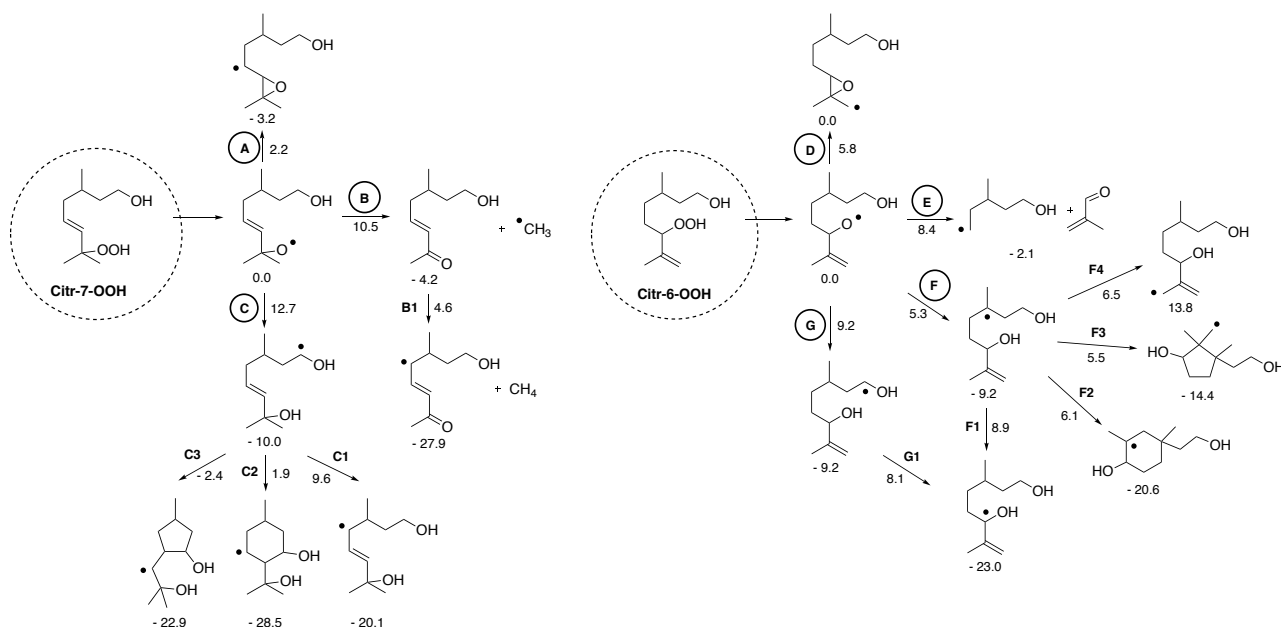
Fig. 4. Preferential paths for the formation of radical intermediates from Citr-7-OOH and Citr-6-OOH according to DFT computational studies. Stereochemistry of chiral centers has not been considered for simplicity reasons. Gibbs energies (ΔG) are given in kcal.mol^{-1}.

3. 4. Reactivity with amino acids

As DFT calculations showed a similar behavior for both Citr-OOHs, we focused the study on single Citr-7-OOH and studied the reactivity with amino acids known to be involved in radical reactions such as cysteine, tyrosine, tryptophan and histidine. We observed the formation of adducts with *N*-acetyl-cysteine methyl ester (*N*-Ac-Cys-COOMe) and *N*-acetyl-histidine methyl ester (*N*-Ac-His-COOMe), while the other amino acids (*N*-Ac-Tyr-COOEt and *N*-Ac-Trp-COOEt) were just oxidized in presence of the hydroperoxide (Supplementary Material S.5).

The reaction of Citr-7-OOH with *N*-Ac-Cys-COOMe in presence of Fe(II) led to the formation of various products within a few hours. LC/ESI-MS analysis of the crude product showed one major peak with associated *m/z* 353, corresponding to the cysteine sulfide dimer, and a second peak with *m/z* 366 (Fig. 5A). ESI-MS/MS of *m/z* 366 showed the release of fragment ions with *m/z* 144 and *m/z* 178 typical from loss of *N*-Ac-Cys-COOMe suggesting the formation of an adduct (Fig. 5B). Mechanistically, the hydroperoxide generates first alkoxyl radicals through oxidation of Fe(II) to Fe(III). These, due to the presence of the allylic double bond, are known to undergo fast cyclization in these experimental conditions affording α-oxiranylcarbinyl radicals that can be trapped by the

lateral chain of cysteine and afford epoxide **4** (Kao et al., 2014). Further addition of a molecule of H$_2$O forms **5** with associated *m/z* 366 (Fig. 5C).
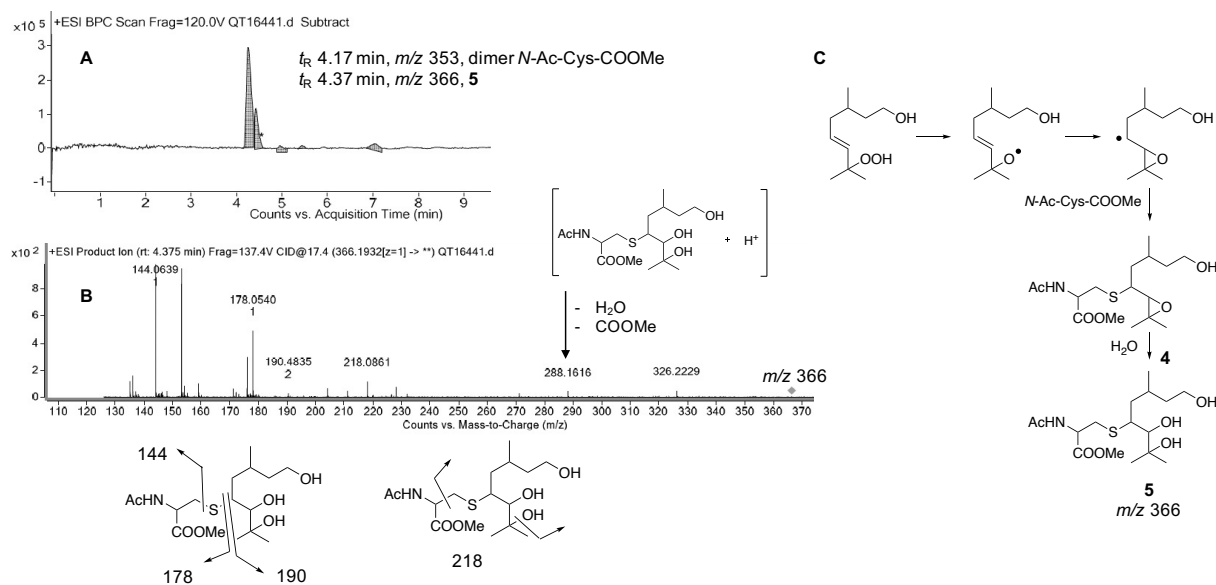

Fig. 5. Reactivity Citr-7-OOH/*N*-Ac-Cys-COOMe/Fe(II). A) LC chromatogram of the crude product; B) MS/MS analysis of peak with associated *m/z* 366; C) Mechanistic pathway for the formation of adduct **5**.

After one week of reaction with *N*-Ac-His-COOMe, Citr-7-OOH was not completely consumed. LC-ESI-MS analysis showed a major peak corresponding to the amino acid with a value of *m/z* 212. In addition, a product with a mass value of *m/z* 382 was detected (Fig. 6A). To deduce a chemical structure compatible with *m/z* 382, a complementary ESI-MS/MS analysis was performed. Release of ions with *m/z* value of 212 characteristic of histidine cleavage were observed together with ions associated with loss of water molecules or groups characteristic of *N*-Ac-His-COOMe, indicating the formation of adducts (Fig. 6B). However, it was not possible to assign a precise chemical structure. Initial alkoxyl radicals can undergo cyclization and oxyranylcarbinyl radicals formed be able to add to histidine and form **6**-like adducts, as it was observed with cysteine. But also, migration of an H atom is favored (Fig.4, path C) and obtained radicals can follow intramolecular cyclisations affording very stable six and/or five member rings C-radicals (Fig. 4, paths C2 and C3). Binding at these C-positions and form **7**-like or **8**-like adducts cannot be thus excluded. Yet, further fragmentation studies did not allow elucidation of the precise position of addition on the side chain of *N*-Ac-His-COOMe.
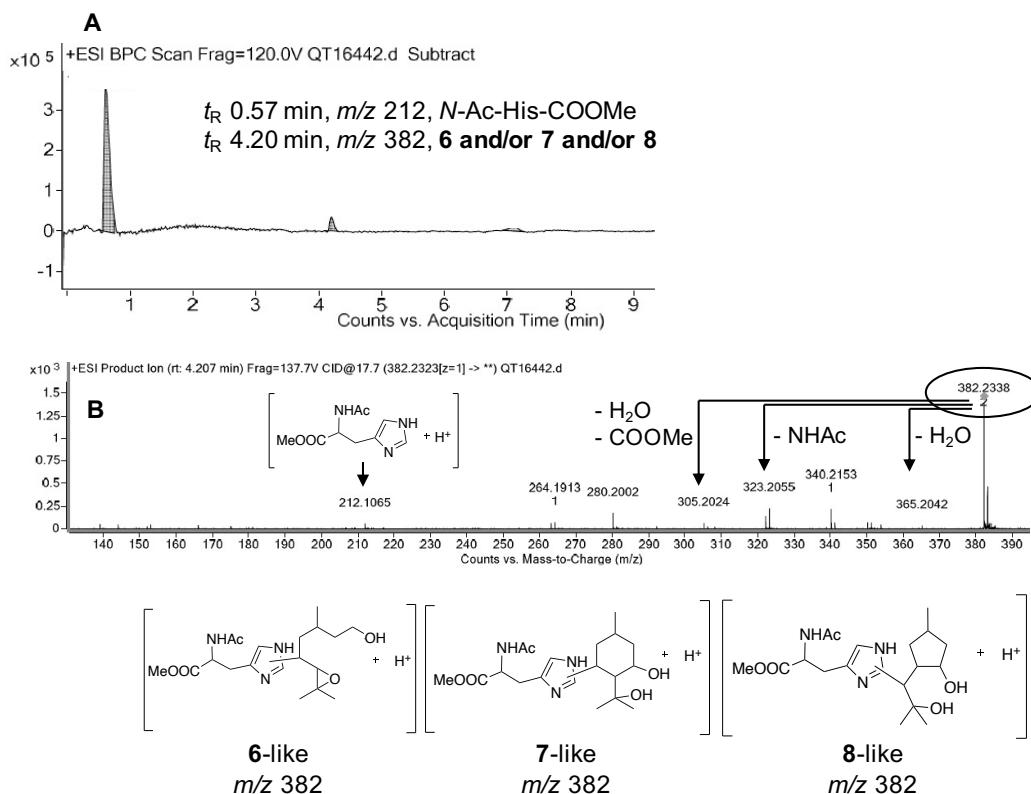
Fig. 6. Reactivity Citr-7-OOH/*N*-Ac-His-COOMe/Fe(II). A) LC chromatogram of the crude product; B) MS/MS analysis of peak with associated *m/z* 382, fitting with adducts **6, 7** and **8**-like

4. Discussion

We report in this manuscript the formation of radical intermediates when exposing topically RHE to Citr-OOHs and their reactivity towards amino acids in solution with the support of DFT studies.

We first investigated by EPR-ST the formation of radicals from a Citr-6-OOH/Citr-7-OOH mixture (6:4 ratio) in a RHE model histologically similar to human skin. In the context of our studies, the availability of RHE models is a great alternative to the use of human or animal tissues, as it amends many legal and ethical issues. The EpiSkin[TM] model we used displays realistic similarities to human epidermis concerning the morphology, the presence of a stratum corneum (penetration concerns), the composition in lipids and the existing biochemical markers (Netzlaff et al., 2005), mimicking thus what may happen *in vivo*. EpiSkin[TM] RHE is moreover more consistent in permeability and responsiveness than human skin which is *per se* highly variable, being thus actually employed for testing skin irritation features of chemicals as replacement of *in vivo* testing (OECD, 2021). The reason we used Citr-6-OOH/Citr-7-OOH mixture (6:4 ratio) is that the first patch testing study with pure and oxidized citronellol reported in the literature in consecutive patients was

performed with a serial dilution of a citronellol autoxidation mixture containing 11.5% (w/w) Citr-6-OOH/Citr-7-OOH in a 6:4 ratio (Hagvall et al., 2020).

EPR-ST preliminary studies in solution gave an overview allowing further characterization of the type of radicals formed in RHE. In the epidermis, both R$^{\bullet}$ (C-centered) and HO$^{\bullet}$ radical DEPMPO spin adducts were identified. Even though Citr-OOHs can release the HO$^{\bullet}$ radical, care must be taken in assigning the signal in aqueous media since side reactions may happen and the radical may not be released from Citr-OOHs but result from the presence of water (Finkelstein et al., 1980; Forrester and Hepburn, 1971). Control experiments however (*i.e.*, incubation with the sole spin trap) gave no signal, suggesting that the competition reaction with water was probably not interfering with trapping of radicals derived from Citr-OOHs.

RHE EPR-ST investigations required higher concentrations of all actors involved compared to studies in solution, in line with the complexity and reductive environment of the system. Fingerprints of the spin adducts characterizing trapped radicals were detected above a 10 mM hydroperoxide threshold and reached a maximum at 50 mM where the best EPR spectra S/N ratios were obtained (Fig. 3). In the patch test study mentioned above, dermatitis consecutive patients were tested with oxidized citronellol (11.5% w/w Citr-OOHs content) at 1%, 2%, 4% or 6% in petrolatum. The authors stated that this corresponded to test, in dose per unit area, approximately 47 $\mu g.cm^{-2}$, 94 $\mu g.cm^{-2}$, 190 $\mu g.cm^{-2}$ or 280 $\mu g.cm^{-2}$ of Citr-OOHs, respectively. In our EPR-ST studies in RHE, topical application of Citr-OOHs 10 mM, 25 mM or 50 mM corresponded to a dose per unit area of approximately 99 $\mu g.cm^{-2}$, 247 $\mu g.cm^{-2}$ or 495 $\mu g.cm^{-2}$, respectively. 99 and 247 $\mu g.cm^{-2}$ are in the range of patch testing patients with 2% (1.7% patients positive) and 6% (4.5% patients positive) air oxidized citronellol. Consequently, in our RHE investigations we come near the elicitation dose per unit area of patch testing to Citr-OOHs, testimony of the EPR-ST high sensitivity to reflect what might happen *in vivo*. Around 247 $\mu g.cm^{-2}$ is the dose per unit area applied to RHE that mimics the best the concentration giving a higher proportion of positive reactions at patch testing.

In a second stage, we investigated in solution if the detected C-radicals were reactive towards amino acids known to participate in radical processes, such as cysteine, histidine, tyrosine and tryptophan. The non-cyclic molecular structure of citronellol is very similar to that of linalool, and upon air exposure it has been shown to follow a similar oxidation pathway (Rudbäck et al., 2014). Hydroperoxides at the 7-position and 6-position are formed for both as primary autoxidation products. Thus, we expected at the beginning a similar reactivity for Citr-OOHs to the one we reported for linalool hydroperoxydes (Lin-OOHs) (Kuresepi et al., 2020). We studied Lin-OOHs reactivity with cysteine by means of ^{13}C-substitution at positions precursor of C-radicals and followed the reactivity by mono- and bidimensional ^{13}C-NMR. As for citronellol, studies were carried out with a mixture Lin-6-OOH/Lin-7-OOH (6:4 ratio) because a linalool oxidation mixture containing both hydroperoxides is currently used in Europe to diagnose by patch testing patients sensitized to Lin-OOHs. Lin-7-OOH seemed to be much more reactive towards cysteine than Lin-6-OOH, and we evidenced that allylic hydrogen abstraction is a major radical pathway to form reactive C-radicals from Lin-7-OOH (Fig. 7).
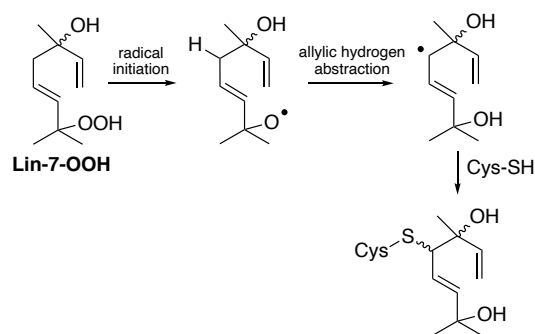

Fig. 7. Formation of a cysteine adduct through the involvement of a C-radical at position 4 of Lin-7-OOH (Kuresepi et al., 2020)

The reactivity of Citr-7-OOH was found to be somehow different suggesting distinct radical-mediated intermediates depending on the chemical structure of the target terpene. Reactivity of Citr-7-OOH towards the thiol group of *N*-Ac-Cys-COOMe was found to be unlike to that of Lin-7-OOH reported previously (Fig. 7). Here, the C-α-oxiranylcarbinyl radical giving adduct **5** was highlighted as good candidate for radical reactive intermediate. This result was supported by DFT studies, the O-radical being basically in equilibrium with the α-oxiranylcarbinyl radical in path A (Fig. 8). This C-

radical position was also reactive toward *N*-Ac-His-COOMe to form adduct **6**-like. Though, Citr-7-OOH reacted also with *N*-Ac-His-COOMe through a radical intermediate similar this time to the one described for Lin-7-OOH, and based on the preliminary abstraction of a hydrogen atom from the formed O-radical (path C). However, while in the case of Lin-7-OOH this abstraction happened on the carbon atom in position 4 in between two favored allylic positions, the absence of the 1,2-double bond of Lin-7-OOH in Citr-7-OOH induces the process on the carbon position in α to the alcohol function. Similar to what it is reported in the literature (Bezard et al., 1997), this last C-radical can lead to the formation of 6- or 5-membered ring systems (paths C2 and C3) and rather stable C-radicals reactive towards the lateral chain of *N*-Ac-His-COOMe affording adducts **7**- and **8**-like respectively. As previously mentioned, based on DFT studies, a similar reactivity might be suspected for Citr-6-OOH.
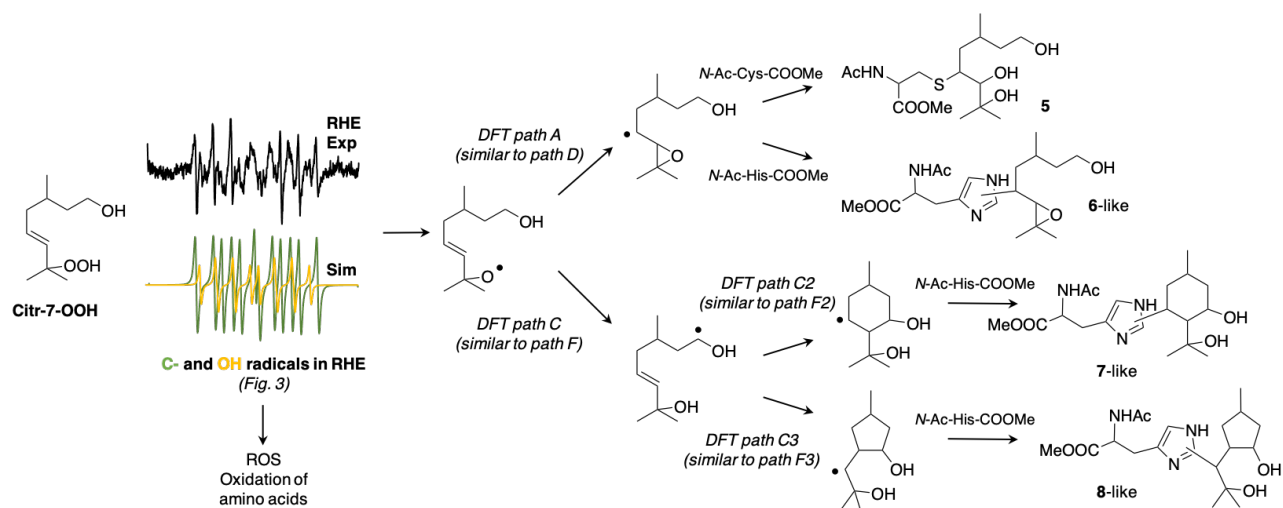

Fig. 8. Citr-7-OOH: formation of C-radicals in RHE and reactivity towards *N*-Ac-Cys/His-COOMe in accordance with DFT studies

We know that a chemical has the potential to induce skin sensitization and become a contact allergen if it is able to react with skin proteins after penetration in the epidermis. A huge progress has been made in the identification of chemical functions present in the molecules related to skin sensitization. The acquired knowledge has been the basis for the establishment of the so-called "structural alerts": the total or partial chemical structures known to present a risk. The presence of such structural alert in a molecule is thus a sign of an aptitude to modify skin proteins and thus act as

a skin sensitizer. A big step forward has been made defining structural alerts in the case of electrophilic compounds reacting with skin proteins through two electrons mechanisms (Lepoittevin and Lafforgue, 2021). The overview of electrophilic reaction mechanisms relevant to skin sensitization and the great number of structure-activity relationships published over the years has led to a classification of allergens according to reaction mechanistic applicability domains (Roberts et al., 2007). This has been used upstream to develop *in chemico* methods to assess the sensitizing potential of chemicals. However, very little has been done to identify structural alerts for skin sensitizers triggering free radical reactions in the skin. Results presented here prove what was suspected for many years, namely that C-radicals that might be responsible for the formation of immunogenic structures depend on the chemical structure of the sensitizing hydroperoxide (*e.g.*, hydrogen abstraction in a specific position in function of the presence of double bonds). This goes hand in hand with previous studies demonstrating that there is no general cross-reactivity between related but different terpene hydroperoxides (Christensson et al., 2006; Karlberg et al., 2008). Thus, it would be possible to start describing structural alerts for molecules reacting through radical mechanisms.

Conclusion

We report here for the first-time studies on the reactivity of Citr-OOHs that might be at the origin of their skin sensitizing behavior. As for various members of the "terpene hydroperoxides" family, the involvement of C-radical intermediates, proved to be formed in RHE, has been evidenced to be again in the first line. Reactivity studies with amino acids ready to react *via* radical mechanisms such as cysteine or histidine have shown that these C-radicals are formed at specific positions pointing out to new radical structural alerts that depend definitely on the molecular structure of the hydroperoxide. The combination of (i) EPR-ST to identify radicals formed in biological tissues, (ii) theoretical DFT studies on preferential paths for radical degradation and (iii) reactivity with amino acids followed by

LC-MS, is thus an efficient toolbox to get insights on radical mechanisms participating in immunogenic hapten-protein interactions.

Acknowledgements

References

Aubry, J.-M., Adam, W., Alsters, P.L., Borde, C., Queste, S., Marko, J., Nardello, V., 2006. Dark singlet oxygenation of organic substrates in single-phase and multiphase microemulsion systems. Tetrahedron 62, 10753–10761. https://doi.org/10.1016/j.tet.2006.08.093

Aubry, J.M., Cazin, B., 1988. Chemical sources of singlet oxygen. 2. Quantitative generation of singlet oxygen from hydrogen peroxide disproportionation catalyzed by molybdate ions. Inorg. Chem. 27, 2013–2014. https://doi.org/10.1021/ic00285a001

Barbati, S., Clément, J.L., Olive, G., Roubaud, V., Tuccio, B., Tordo, P., 1997. 31P Labeled cyclic nitrones: A new class of spin traps for free radicals in biological milieu, in: Minisci, F. (Ed.), Free Radicals in Biology and Environment. Springer Netherlands, Dordrecht, pp. 39–47. https://doi.org/10.1007/978-94-017-1607-9_3

Basketter, D.A., Alépée, N., Ashikaga, T., Barroso, J., Gilmour, N., Goebel, C., Hibatallah, J., Hoffmann, S., Kern, P., Martinozzi-Teissier, S., Maxwell, G., Reisinger, K., Sakaguchi, H., Schepky, A., Tailhardat, M., Templier, M., 2014. Categorization of chemicals according to their relative human skin sensitizing potency. Dermatitis 25, 11–21. https://doi.org/10.1097/DER.0000000000000003

Bezard, M., Karlberg, A.-T., Montelius, J., Lepoittevin, J.-P., 1997. Skin sensitization to linalyl hydroperoxide: support for radical intermediates. Chem. Res. Toxicol. 10, 987–993. https://doi.org/10.1021/tx970014r

Christensson, J.B., Matura, M., Bäcktorp, C., Börje, A., Nilsson, J.L.G., Karlberg, A.-T., 2006. Hydroperoxides form specific antigens in contact allergy. Contact Dermatitis 55, 230–237. https://doi.org/10.1111/j.1600-0536.2006.00913.x

Cossi, M., Barone, V., Cammi, R., Tomasi, J., 1996. Ab initio study of solvated molecules: a new implementation of the polarizable continuum model. Chem. Phys. Letters 255, 327–335. https://doi.org/10.1016/0009-2614(96)00349-1

Dikalov, S., Tordo, P., Motten, A., Mason, R.P., 2003. Characterization of the high resolution ESR spectra of the methoxyl radical adducts of 5-(diethoxyphosphoryl)-5-methyl-1-pyrroline *N*-oxide (DEPMPO). Free Radic. Res. 37, 705–712. https://doi.org/10.1080/1071576031000097508

Ditchfield, R., Hehre, W.J., Pople, J.A., 1971. Self-consistent molecular-orbital methods. IX. An extended gaussian-type basis for molecular-orbital studies of organic molecules. J. Chem. Phys. 54, 724–728. https://doi.org/10.1063/1.1674902

EC, 2009. Regulation (EC) No. 1223/2009 of the European Parliament and of the Council of 30 novemeber 2009 on cosmetic products. Off. J. Eur. Union L342, 59–209.

Finkelstein, E., Rosen, G.M., Rauckman, E.J., 1980. Spin trapping of superoxide and hydroxyl radical: Practical aspects. Arch. Biochem. Biophys. 200, 1–16. https://doi.org/10.1016/0003-9861(80)90323-9

Forrester, A.R., Hepburn, S.P., 1971. Spin traps. A cautionary note. J. Chem. Soc., C 701. https://doi.org/10.1039/j39710000701

Frejaville, C., Karoui, H., Tuccio, B., Moigne, F.L., Culcasi, M., Pietri, S., Lauricella, R., Tordo, P., 1995. 5-(Diethoxyphosphoryl)-5-methyl-1-pyrroline N-oxide: a new efficient phosphorylated nitrone for the in vitro and in vivo spin trapping of oxygen-centered radicals. J. Med. Chem. 38, 258–265. https://doi.org/10.1021/jm00002a007

Frosch, P.J., Pirker, C., Rastogi, S.C., Andersen, K.E., Bruze, M., Svedman, C., Goossens, A., White, I.R., Uter, W., Arnau, E.G., Lepoittevin, J.-P., Menne, T., Johansen, J.D., 2005a. Patch testing with a new fragrance mix detects additional patients sensitive to perfumes and missed by the current fragrance mix. Contact Dermatitis 52, 207–215. https://doi.org/10.1111/j.0105-1873.2005.00565.x

Frosch, P.J., Rastogi, S.C., Pirker, C., Brinkmeier, T., Andersen, K.E., Bruze, M., Svedman, C., Goossens, A., White, I.R., Uter, W., Arnau, E.G., Lepoittevin, J.-P., Johansen, J.D., Menne, T., 2005b. Patch testing with a new fragrance mix - reactivity to the individual constituents and chemical detection in relevant cosmetic products. Contact Dermatitis 52, 216–225.

https://doi.org/10.1111/j.0105-1873.2005.00563.x

Hagvall, L., Rudbäck, J., Bråred Christensson, J., Karlberg, A., 2020. Patch testing with purified and oxidized citronellol. Contact Dermatitis 83, 372–379. https://doi.org/10.1111/cod.13654

Kao, D., Chaintreau, A., Lepoittevin, J.-P., Giménez-Arnau, E., 2014. Mechanistic studies on the reactivity of sensitizing allylic hydroperoxides: investigation of the covalent modification of amino acids by carbon-radical intermediates. Toxicol. Res. 3, 278. https://doi.org/10.1039/c3tx50109d

Kao, D., Chaintreau, A., Lepoittevin, J.-P., Giménez-Arnau, E., 2011. Synthesis of allylic hydroperoxides and EPR spin-trapping studies on the formation of radicals in iron systems as potential initiators of the sensitizing pathway. J. Org. Chem. 76, 6188–6200. https://doi.org/10.1021/jo200948x

Karlberg, A.-T., Bergström, M.A., Börje, A., Luthman, K., Nilsson, J.L.G., 2008. Allergic Contact Dermatitis—Formation, Structural Requirements, and Reactivity of Skin Sensitizers. Chem. Res. Toxicol. 21, 53–69. https://doi.org/10.1021/tx7002239

Karlberg, A.-T., Börje, A., Duus Johansen, J., Lidén, C., Rastogi, S., Roberts, D., Uter, W., White, I.R., 2013. Activation of non-sensitizing or low-sensitizing fragrance substances into potent sensitizers - prehaptens and prohaptens. Contact Dermatitis 69, 323–334. https://doi.org/10.1111/cod.12127

Karoui, H., Chalier, F., Finet, J.-P., Tordo, P., 2011. DEPMPO: an efficient tool for the coupled ESR-spin trapping of alkylperoxyl radicals in water. Org. Biomol. Chem. 9, 2473. https://doi.org/10.1039/c0ob00876a

Kuresepi, S., Vileno, B., Lepoittevin, J.-P., Giménez-Arnau, E., 2020. Mechanistic insights on skin sensitization to linalool hydroperoxides: EPR evidence on radical intermediates formation in reconstructed human epidermis and ^{13}C NMR reactivity studies with thiol residues. Chem. Res. Toxicol. 33, 1922–1932. https://doi.org/10.1021/acs.chemrestox.0c00125

Kuresepi, S., Vileno, B., Turek, P., Lepoittevin, J.-P., Giménez-Arnau, E., 2018. Potential of EPR spin-trapping to investigate *in situ* free radicals generation from skin allergens in reconstructed human epidermis: cumene hydroperoxide as proof of concept. Free Radic. Res. 52, 171–179. https://doi.org/10.1080/10715762.2017.1420906

Lauricella, R., Tuccio, B., 2020. Detection and characterisation of free radicals after spin trapping, in: Electron Paramagnetic Resonance Spectroscopy. Springer International Publishing, Cham, pp. 51–82. https://doi.org/10.1007/978-3-030-39668-8_3

Lepoittevin, J.-P., Karlberg, A.-T., 1994. Interactions of allergenic hydroperoxides with proteins: a radical mechanism? Chem. Res. Toxicol. 7, 130–133. https://doi.org/10.1021/tx00038a003

Lepoittevin, J.-P., Lafforgue, C., 2021. Molecular aspects in allergic and irritant contact dermatitis, in: Johansen, J.D., Mahler, V., Lepoittevin, J.-P., Frosch, P.J. (Eds.), Contact Dermatitis. Springer International Publishing, Cham, pp. 121–138. https://doi.org/10.1007/978-3-030-36335-2_4

Lichter, J., Silva e Sousa, M., Peter, N., Sahli, F., Vileno, B., Kuresepi, S., Gourlaouen, C., Giménez-Arnau, E., Blömeke, B., 2021. Skin sensitization to fragrance hydroperoxides: interplay between dendritic cells, keratinocytes and free radicals. Br. J. Dermatol. 184, 1143–1152. https://doi.org/10.1111/bjd.19685

Martin, S.F., 2015. Immunological mechanisms in allergic contact dermatitis. Curr. Opin. Allergy Clin. Immunol. 15, 124–130. https://doi.org/10.1097/ACI.0000000000000142

Netzlaff, F., Lehr, C.-M., Wertz, P.W., Schaefer, U.F., 2005. The human epidermis models EpiSkin®, SkinEthic® and EpiDerm®: An evaluation of morphology and their suitability for testing phototoxicity, irritancy, corrosivity, and substance transport. Eur. J. Pharm. Biopharm. 60, 167–178. https://doi.org/10.1016/j.ejpb.2005.03.004

OECD, 2021. OECD Guidelines for theTesting of Chemicals. Test No. 439.Section 4. In vitro skin irritation: reconstructed human epidermis test method. OECD Publishing Paris. https://doi.org/10.1787/9789264242845-en

OECD, 2014. OECD Series on Testing and Assessment. No. 168. The Adverse Outcome Pathway for skin sensitization initiated by covalent binding to proteins. Editions OECD, Paris.

https://doi.org/10.1787/20777876

Panico, A., Serio, F., Bagordo, F., Grassi, T., Idolo, A., De Giorgi, M., Guido, M., Congedo, M., De Donno, A., 2019. Skin safety and health prevention: an overview of chemicals in cosmetic products. J. Prev. Med. Hyg. Vol 60, E50–E57. https://doi.org/10.15167/2421-4248/JPMH2019.60.1.1080

Rastogi, S.C., Heydorn, S., Johansen, J.D., Basketter, D.A., 2001. Fragrance chemicals in domestic and occupational products. Contact Dermatitis 45, 221–225. https://doi.org/10.1034/j.1600-0536.2001.450406.x

Roberts, D.W., Aptula, A.O., Patlewicz, G., 2007. Electrophilic chemistry related to skin sensitization. Reaction mechanistic applicability domain classification for a published data set of 106 chemicals tested in the mouse local lymph node assay. Chem. Res. Toxicol. 20, 44–60. https://doi.org/10.1021/tx060121y

Rudbäck, J., Hagvall, L., Börje, A., Nilsson, U., Karlberg, A.-T., 2014. Characterization of skin sensitizers from autoxidized citronellol - impact of the terpene structure on the autoxidation process. Contact Dermatitis 70, 329–339. https://doi.org/10.1111/cod.12234

Sahli, F., Godard, A., Vileno, B., Lepoittevin, J.-P., Giménez-Arnau, E., 2019a. Formation of methyl radicals derived from cumene hydroperoxide in reconstructed human epidermis: an EPR spin trapping confirmation by using [13] C-substitution. Free Radic. Res. 53, 737–747. https://doi.org/10.1080/10715762.2019.1624741

Sahli, F., Sousa, M.S.E., Vileno, B., Lichter, J., Lepoittevin, J.-P., Blömeke, B., Giménez-Arnau, E., 2019b. Understanding the skin sensitization capacity of ascaridole: a combined study of chemical reactivity and activation of the innate immune system (dendritic cells) in the epidermal environment. Arch. Toxicol. 93, 1337–1347. https://doi.org/10.1007/s00204-019-02444-3

Santos, P.L., Matos, J.P.S.C.F., Picot, L., Almeida, J.R.G.S., Quintans, J.S.S., Quintans-Júnior, L.J., 2019. Citronellol, a monoterpene alcohol with promising pharmacological activities - A systematic review. Food Chem. Toxicol. 123, 459–469. https://doi.org/10.1016/j.fct.2018.11.030

Sharpless, K.B., Lauer, R.F., 1973. Mild procedure for the conversion of epoxides to allylic alcohols. First organoselenium reagent. J. Am. Chem. Soc. 95, 2697–2699. https://doi.org/10.1021/ja00789a055

Soo Lim, D., Min Choi, S., Kim, K.-B., Yoon, K., Kacew, S., Sik Kim, H., Lee, B.-M., 2018. Determination of fragrance allergens and their dermal sensitization quantitative risk assessment (QRA) in 107 spray perfumes. J. Toxicol. Environ. Health, Part A 81, 1173–1185. https://doi.org/10.1080/15287394.2018.1543232

Stoll, S., Schweiger, A., 2006. EasySpin, a comprehensive software package for spectral simulation and analysis in EPR. J Magn Reson 178, 42–55. https://doi.org/10.1016/j.jmr.2005.08.013

Vileno, B., Port-Lougarre, Y., Giménez-Arnau, E., 2022. Electron paramagnetic resonance and spin trapping to detect free radicals from allergenic hydroperoxides in contact with the skin: From the molecule to the tissue. Contact Dermatitis cod.14037. https://doi.org/10.1111/cod.14037

Wieck, S., Olsson, O., Kümmerer, K., Klaschka, U., 2018. Fragrance allergens in household detergents. Regul. Toxicol. Pharmacol. 97, 163–169. https://doi.org/10.1016/j.yrtph.2018.06.015